

Biocompatible Drug Delivery System Based on a MOF Platform for a Sustained and Controlled Release of the Poorly Soluble Drug Norfloxacin

Preeti Yadav, Sarita Kumari, Anand Yadav, Priya Bhardwaj, Mulaka Maruthi, Anindita Chakraborty,* and Prakash Kanoo*



Cite This: *ACS Omega* 2023, 8, 28367–28375



Read Online

ACCESS |



Metrics & More

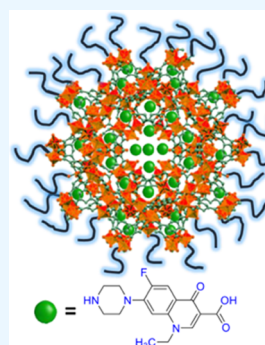


Article Recommendations

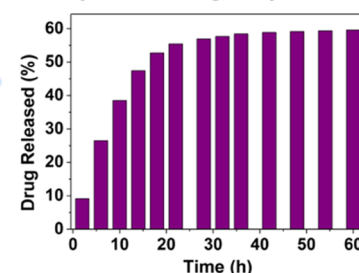


Supporting Information

ABSTRACT: Norfloxacin (NFX), an important antibacterial fluoroquinolone, is a class IV drug according to the biopharmaceutics classification system (BCS) and has low solubility and permeability issues. Such poor physicochemical properties of drug molecules lead to poor delivery and are of serious concern to the pharmaceutical industry for clinical development. We present here a conceptually new approach to deliver NFX, by loading the drug molecule on the porous platform of a biocompatible metal–organic framework (MOF), MIL-100(Fe). The loading of the drug on the MOF leading to NFX@MIL-100(Fe) was characterized by Fourier transform infrared (FTIR), UV–visible spectroscopy, thermogravimetric analyses (TGA), and nitrogen adsorption studies. Controlled experiments resulted in the high loading of the drug molecule (~20 wt %) along with the desired sustained release. We could further control the release of norfloxacin by coating drug-loaded MIL-100(Fe) with PEG, PEG{NFX@MIL-100(Fe)}. Both drug delivery systems (DDSs), NFX@MIL-100(Fe) and PEG{NFX@MIL-100(Fe)}, were tested for their biocompatibility through toxicity studies. The DDSs are biocompatible and show insignificant cytotoxicity, as revealed by cell viability studies through the 3-(4,5-dimethylthiazol-2-yl)-2,5-diphenyltetrazolium bromide (MTT) assay.



Sustained and Controlled Release of Poorly Soluble Drug, Norfloxacin



1. INTRODUCTION

Drug delivery systems that comprise metal–organic frameworks (MOFs) as carriers or vehicles have proven to be attractive over the years and several researchers have reported cases with a focus on drug loading and delivery.^{1–7} It is equally interesting to realize that MOFs are excellent platforms for a sustained and controlled release of drug molecules, and the property is potentially demanding for those drugs in the pharmaceutical industry that face major formulation-related problems of low water solubility,^{8,9} thus leading to the decreased bioavailability of active pharmaceutical ingredients (APIs). It is not surprising that the focus has shifted to the latter with new investigations, if not too many, emerging on the sustained and controlled release of drugs from MOF-based drug delivery systems (DDSs).^{10–19}

MOFs are hybrid crystalline materials that consist of cationic metal nodes and anionic/neutral organic linkers connected via coordination bonds expanding in three dimensions.^{20–22} The high pore volume and surface area of MOFs have attracted researchers from all over the world, enabling their use in various applications, namely, gas storage,^{23,24} catalysis,^{25,26} dye adsorption,²⁷ drug delivery,^{1–7,10–19} etc. Many MOFs possess a variety of biological applications aided by (i) biocompati-

bility, biodegradability, and nontoxicity;²⁸ (ii) facile surface chemistry that allows conjugation of various functionalities;¹⁶ (iii) the ability to load a variety of cargos;^{17,29–31} (iv) stability within the gastrointestinal tract; etc.³² These properties of MOFs make them ideal candidates to be used as potential DDSs.

Norfloxacin (NFX) is an important antibacterial fluoroquinolone drug that belongs to class IV of the biopharmaceutics classification system (BCS) and faces issues of low aqueous solubility and permeability.⁹ To achieve the desired bioavailability, the release of NFX in biological systems should be sustained and controlled. Several approaches have been employed in the past to address the release and bioavailability issue of NFX in aqueous media.^{9,33–37} Crystal engineers use a cocrystallization approach to increase the solubility of

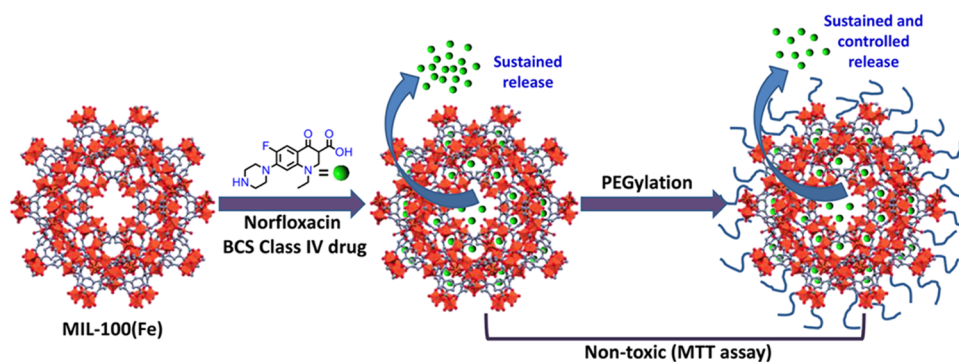
Received: April 10, 2023

Accepted: July 14, 2023

Published: July 27, 2023



Scheme 1. Schematic Showing the Loading of NFX in MIL-100(Fe) and Its Subsequent Release from MIL-100(Fe) and PEG-Coated MIL-100(Fe)



norfloxacin.^{9,33} Drug salt formulation is also proposed with many carboxylic acids;^{34,35} however, preserving the therapeutic benefit has been challenging. Therefore the search for a DDS that shows an effective and efficient release of NFX in a sustained and controlled manner and is easily processable is highly desirable. Although several drugs have been loaded on various MOFs,^{1–7,10–19} norfloxacin loading and its release from MOFs have not been studied and reported to date. During our experiments in the laboratory, we have observed that norfloxacin is a notorious drug molecule, as it rapidly precipitates out in aqueous media even at very low concentrations (0.40 mg mL⁻¹ at pH 7 and 0.45 mg mL⁻¹ at pH 7.5). This observation augments the classification of the drug as class IV in BCS. In this contribution, we have come up with an idea of delivering norfloxacin in a sustained and controlled fashion by loading it into the porous nanochannels of a biocompatible MOF (Scheme 1). Such confinement into a porous platform resulted in a sustained release of the drug. Further, controlled release was achieved by coating the drug-loaded MOF with poly(ethylene glycol) (PEG). The sustained and controlled release in a simulated physiological condition (phosphate buffer solution, PBS) will keep the local concentration of the drug in PBS media low and, therefore, will not allow the drug molecules to precipitate rapidly. The incremental release of the drug for several hours will ensure efficient delivery. Further, this ensures a decrease in the loss of the drug during the entire delivery process and therefore makes the DDS economical (Scheme S1).

2. EXPERIMENTAL METHODS

2.1. Materials. All reagents and solvents used were commercially available and used as such without any further purification. Ferric chloride hexahydrate (FeCl₃·6H₂O), trimesic acid (C₉H₆O₆), terephthalic acid (C₈H₆O₄), and 2-aminoterephthalic acid (C₈H₄NO₄) were obtained from Sigma-Aldrich Chemical Company. Poly(ethylene glycol) (PEG-400 for synthesis) and sodium hydroxide pellets purified (NaOH) were obtained from Central Drug House (CDH), Delhi. Norfloxacin (C₁₆H₁₈FN₃O₃) was obtained from Yarrow Chem Products Company, Mumbai. Potassium dihydrogen phosphate (KH₂PO₄) was obtained from Emplura, Mumbai.

2.2. Physical Measurements. Functional groups were characterized by Fourier transform infrared spectroscopy (FTIR) recorded on a Bruker IFS 66v/S spectrophotometer in the region of 4000–600 cm⁻¹. Drug encapsulation in the MOF was also identified via FTIR spectroscopy. The crystallinity and phase purity of MIL-100(Fe) was measured

by powder X-ray diffraction (PXRD) over the 2θ range of 5–50° and recorded on a Bruker D8 Discover instrument using Cu Kα radiation. Loading and release studies of the drug were carried out using UV–vis spectroscopy. UV–vis absorption spectra were recorded on a Shimadzu UV-2600 spectrophotometer using quartz cells (10 mm × 4 mm light path). Thermogravimetric analyses (TGA) of the samples were performed using a Simultaneous Thermal Analyzer SDT650 unit heated from room temperature to 500 °C at a heating rate of 5 °C min⁻¹ under a flowing nitrogen atmosphere. N₂ adsorption–desorption measurements at 77 K were carried out using a Quantachrom Autosorb IQ-C and a Nova Series-Nova 800. Field emission scanning electron microscopy was employed to analyze the morphology of the samples using a 7610F Plus/JEOL.

2.3. Cytotoxicity Test. The cytotoxicity of NFX-loaded MIL-100(Fe) was analyzed using a 3-(4,5-dimethylthiazol-2-yl)-2,5-diphenyltetrazolium bromide (MTT) assay of cellular activity on Vero-2 cells. The Vero-2 cells were cultured in Dulbecco's modified Eagle medium (DMEM; Gibco by Life Technologies) containing 10% FBS, antibiotics (10,000 U/mL penicillin; 10,000 μg/mL streptomycin) at 37 °C with 5% CO₂ conditions. The culture media was changed every 24 h, and cell recovery was done by trypsinization with 0.25% trypsin-EDTA.

2.4. Synthesis of MIL-100(Fe). MIL-100(Fe) was synthesized from a mixture of ferric chloride hexahydrate (4 mmol), trimesic acid (4 mmol), and 1:1 (v/v) mixture of water and ethanol (20 mL) following a reported procedure.²⁷ Briefly, trimesic acid was taken in 20 mL of a solution of water and ethanol, and to this, FeCl₃·6H₂O was added with continuous stirring till the solution became colloidal. The solution was then transferred to a Teflon-lined steel autoclave and reacted at 140 °C for 12 h. After cooling, the product was obtained by centrifugation and washed 3 times each with ethanol and water to remove unreacted reactants. The resulting product was dried under vacuum for 12 h.

2.5. Encapsulation of Norfloxacin (NFX) in MIL-100(Fe). Prior to encapsulation of the drug, MOF was activated under vacuum at 120 °C for 14 h to evacuate the guest molecules from pores. For loading of NFX in MIL-100(Fe), NFX and MIL-100(Fe) were taken in a 3:1 molar ratio. NFX was dissolved in acetonitrile solvent with the assistance of heat. This solution was then added to the dehydrated MOF and kept at 82 °C for 60 h with continuous stirring (600 rpm). The resulting product, NFX@MIL-100(Fe), was obtained by centrifugation and washed three

times with acetonitrile to remove unreacted NFX, if any, and then dried under vacuum.

2.6. Optimization of NFX Loading. To calculate the total amount of NFX loaded in MOF, first, the sample was digested in an acidic buffer by adding 10 mg of the sample to 10 mL of PBS solution and then adding few drops of concentrated HCl to it. After complete degradation of the sample, its UV–vis spectrum was taken by taking 100 μ L of stock solution and then diluting it with 3 mL of buffer. The amount of drug loaded was then calculated following the Beer–Lambert Law from the absorbance at 272 nm.

2.7. In Vitro NFX Release Study. An NFX release study was carried out according to a reported procedure.^{38,39} 10 mg of PEG{NFX@MIL-100(Fe)} was suspended in 10 mL of phosphate buffer solution (PBS) of pH 7.4 at 37 °C. All of the experiments were carried out in an incubator with a shaking speed of 100 rpm. By measuring the UV–vis absorbance of the supernatant in PBS at regular time intervals, the amount of drug release was calculated. The PBS solution was decanted from the composites at each testing interval via centrifugation at 10,000 rpm for 10 min. This was replaced by an equal amount of fresh PBS after each testing and the procedure was continued till a saturation in release was obtained. NFX concentration in the supernatant was identified by UV–vis absorbance at 272 nm. The absorption coefficient of NFX was measured from the slope of the absorbance versus concentration plot of five known concentration solutions of NFX in PBS of pH 7.4 and measured at 272 nm by a UV–vis spectrophotometer.

2.8. Coating of NFX@MIL-100(Fe) with PEG. The coating was done according to a reported procedure.⁴⁰ 100 mg of NFX@MIL-100(Fe) was first dispersed in a 1:1 v/v mixture of water and ethanol (10 mL), and to this, 5 mL of PEG was added, and the resulting mixture was sonicated for 10 min. The resulting product was obtained by centrifugation at 10,000 rpm for 10 min and washed three times each with ethanol and water. The product was then dried under vacuum for 8 h. The successful coating of PEG on NFX@MIL-100(Fe) was confirmed by FTIR spectroscopy. The coated sample, hereafter, would be designated as PEG{NFX@MIL-100(Fe)}.

2.9. Synthesis of MIL-53. MIL-53(Fe) was synthesized from a mixture of ferric chloride hexahydrate (1 mmol) and terephthalic acid (1 mmol) in 5 mL of DMF following a reported procedure.⁶ Briefly, the solution mixture was first sonicated for 10 min and then transferred to a Teflon-lined steel autoclave and reacted at 150 °C for 2 h. After cooling, the product was obtained by centrifugation at 5000 rpm for 10 min and washed 3 times with DMF to remove unreacted reactants. The solvent was removed by dispersing 100 mg of the obtained product in 200 mL of deionized water and afterward centrifuged to obtain the product.

2.10. Synthesis of MIL-101(Fe)_NH₂. MIL-101(Fe)_NH₂ was synthesized from a mixture of ferric chloride hexahydrate, 2-aminoterephthalic acid (NH₂-H₂BDC), and dimethylformamide (DMF) following a reported procedure.⁶ Briefly, 1.242 mmol of NH₂-H₂BDC was dissolved in 7.5 mL of DMF, and to this, a solution of 2.497 mmol of FeCl₃·6H₂O in 7.5 mL of DMF was added. The solution was then transferred to a Teflon-lined steel autoclave and reacted at 110 °C for 24 h. The product was obtained by centrifugation and washed 3 times each with DMF to remove unreacted reactants. The resulting product was dried under vacuum.

2.11. Encapsulation of NFX in MIL-53(Fe). To encapsulate NFX in MIL-53(Fe), the MOF was heat activated under vacuum at 150 °C for 12 h to evacuate the guest molecules from pores. The method mentioned in Section 2.5 was followed for the encapsulation of NFX in MIL-53(Fe).

2.12. Encapsulation of NFX in MIL-101(Fe)_NH₂. Prior to encapsulation of the drug, the MOF was heat activated under vacuum at 150 °C for 12 h to evacuate the guest molecules from pores. The method mentioned in Section 2.5 was followed for the encapsulation of NFX in MIL-101(Fe)_NH₂.

3. RESULTS AND DISCUSSION

3.1. Synthesis and Characterization of MIL-100(Fe).

To realize a sustained and controlled release of NFX from a MOF, we have judiciously selected the popular Fe-based biocompatible MOF, MIL-100(Fe) constituting Fe₃O trimers and the BTC³⁻ (1,3,5-benzene tricarboxylate) linker as the drug delivery vehicle.^{1,6,7,14,17,29–31} MIL-100(Fe) has good thermal and chemical stability along with its nontoxicity and biocompatibility, which has made it a popular choice for the efficient delivery of several drug molecules. It possesses two kinds of mesocages of sizes \sim 25 and \sim 29 Å accessible through two types of windows, a pentagonal (\sim 4.8 Å \times 5.8 Å) and a hexagonal (\sim 8.6 Å), and has a high surface area.^{1,5} MIL-100(Fe) was synthesized following a reported procedure.²⁷ The MOF was characterized by PXRD, IR, and TGA studies (Figures 1, S1, and S2). The characterization indicates

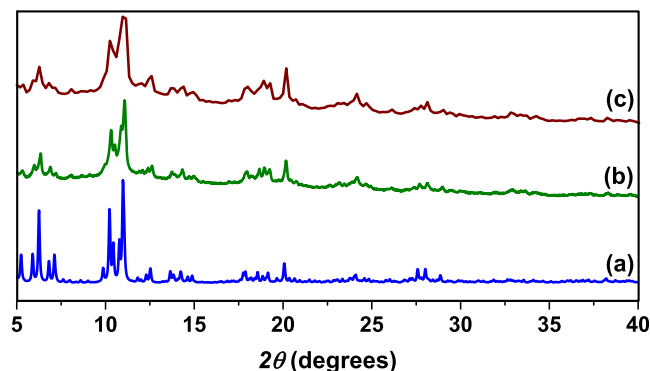


Figure 1. PXRD pattern recorded at various stages. (a) Simulated PXRD patterns of MIL-100(Fe) and (b) as-synthesized patterns of MIL-100(Fe) and (c) NFX@MIL-100(Fe).

formation of the pure phase of the MOF, and the PXRD and IR results match well with the literature. In the PXRD pattern, the peaks in NFX@MIL-100(Fe) are slightly broadened and are not uncommon for MIL-100(Fe) after drug loading. However, importantly, the 2θ positions match well with the as-synthesized pattern.

3.2. Encapsulation of NFX in MIL-100(Fe). Our work started with the synthetic challenge to effectively load the poorly soluble drug, NFX into the selected MIL-100 (Fe) MOF. To load NFX in MIL-100(Fe), several solvents were screened at various temperatures and the best results with the highest loading were obtained in acetonitrile medium at 80 °C. The presence of the characteristic peaks of NFX in the FTIR spectrum of NFX-loaded MIL-100(Fe), NFX@MIL-100(Fe), confirms the successful encapsulation of the drug in the MOF (Figures 2, S3, and S4). The most characteristic peak of the drug, ν C=O, appears at 1714 cm^{-1} in the NFX@MIL-

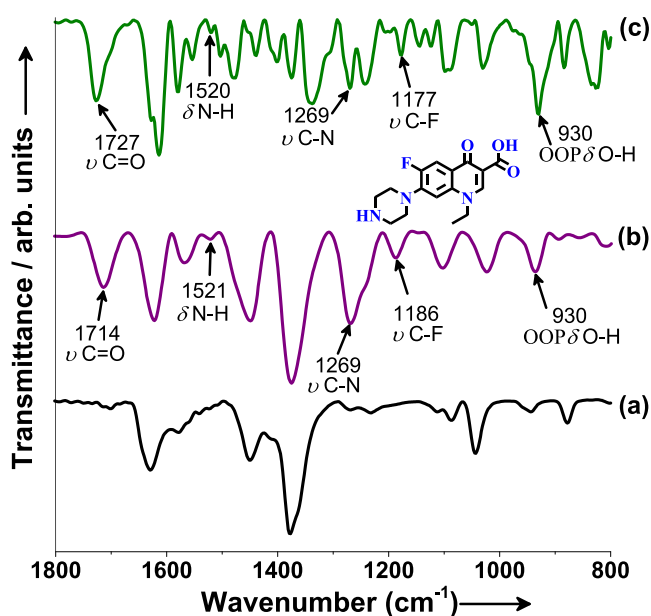


Figure 2. FTIR spectra recorded at various stages: (a) MIL-100(Fe), (b) NFX@MIL-100(Fe), and (c) NFX. The signatures of NFX in NFX@MIL-100(Fe) suggest the successful loading of NFX in MIL-100(Fe).

100(Fe) sample compared to that appearing at 1727 cm^{-1} in the pristine NFX. Such a downshift of the $\nu\text{C}=\text{O}$ stretching mode suggests a favorable interaction of the drug through its carboxylate group with the MOF and may be related to some weak coordinative interaction with Fe(III) centers.⁷ The N–H bending peak at 1521 cm^{-1} , C–N stretching vibration at around 1269 cm^{-1} , C–F stretching vibration at 1186 cm^{-1} , and O–H out of plane bending vibration at 930 cm^{-1} in NFX@MIL-100(Fe) further confirm the occlusion of NFX in MIL-100(Fe). To further validate the encapsulation of NFX in the pore of MIL-100(Fe), we have carried out the nitrogen adsorption studies of MIL-100(Fe) and NFX@MIL-100(Fe). The adsorption isotherms are shown in Figure 3. The

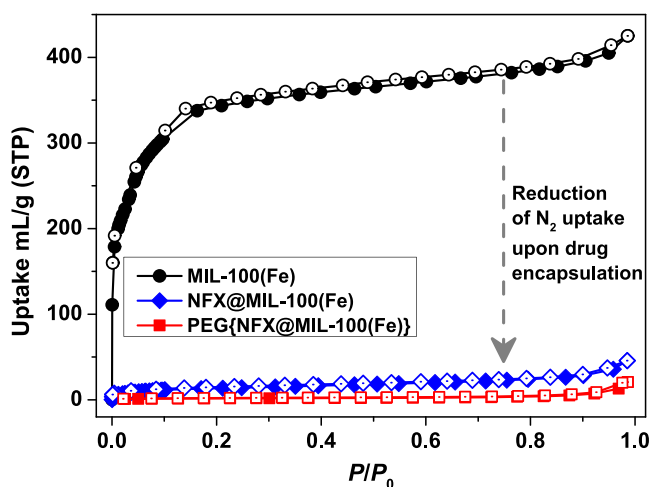


Figure 3. Nitrogen adsorption isotherms measured at 77 K for MIL-100(Fe) (black), NFX@MIL-100(Fe) (blue), and PEG{NFX@MIL-100(Fe)} (red). Closed symbols indicate adsorption and open symbols desorption. P_0 is the saturated vapor pressure of the adsorbates at the measurement temperatures.

Brunauer–Emmett–Teller (BET) surface area calculated for MIL-100(Fe) turns out to be $1377.8\text{ m}^2\text{ g}^{-1}$, which decreases drastically to $52.5\text{ m}^2\text{ g}^{-1}$ in the case of NFX@MIL-100(Fe). This clearly suggests that the pores in MIL-100(Fe) are occupied by NFX molecules in NFX@MIL-100(Fe).

The stability of the MOF after loading of NFX was confirmed by PXRD and TGA studies (Figures 1 and S2). The similarity in peak positions in the XRD pattern confirms that the MOF structure remains intact after the entrapment of NFX in MIL-100(Fe). Also, from the TGA profile, it appears that the stability of the MOF remains intact even after NFX loading. As-synthesized MIL-100(Fe) particles are in a nanoscale region with around 100–500 nm particle size. However, the morphology of the particles is different from the previously reported faceted morphology of the nanoparticles (Figure 4).⁴¹ Such a difference is due to the different synthetic methods we have adapted in our synthetic procedure. After NFX incorporation, we do not observe any visible changes in the morphology of NFX-encapsulated MIL-100(Fe) from the as-synthesized one, which also presents a nanoscale morphology. However, some aggregation of particles has been observed after coating the surface of NFX-encapsulated MOF with PEG, which may be due to the adhesive nature of PEG, acting as glue by coating the particles.

Total drug loading was calculated by digesting NFX@MIL-100(Fe) in PBS of pH 7.4 with the aid of few drops of HCl for 24 h. The amount of NFX released was measured with the help of UV–vis spectroscopy at $\lambda_{\text{max}} 272\text{ nm}$. A calibration curve obtained from five known concentration solutions of NFX in phosphate buffer of pH 7.4 was used to calculate the molar extinction coefficient (Figure S5). MIL-100(Fe) shows a high drug loading capacity wherein 200 mg of NFX is loaded per gram of the MOF (Figure S6). The total amount of drug load has also been calculated through TGA, and it is found that 19.9% of NFX has been encapsulated in MIL-100(Fe), which is quite comparable with the UV result. We have also screened other potential MOFs, MIL-53(Fe)⁶ and NH_2 -functionalized MIL-101(Fe), MIL-101(Fe)- NH_2 ,⁴² for NFX loading under similar conditions (Figures S7 and S8). It is worth mentioning that in comparison to MIL-100(Fe), MIL-53 and MIL-101(Fe)- NH_2 show much lower drug loadings of 6.1 and 9.7%, respectively (Figure 5). High drug encapsulation efficiency (20%) in the case of MIL-100(Fe) might be attributed to the large pore volume and wide internal surface area of the MOF. The driving force for the successful occlusion of NFX in MIL-100(Fe) is possibly due to the favorable noncovalent interactions, including hydrogen bonding between the $-\text{C}=\text{O}$, $-\text{COOH}$, and $-\text{N}-\text{H}$ groups of NFX and $-\text{O}-\text{H}$ and $-\text{COO}^-$ groups of MIL-100(Fe).^{5,19} The drug loading percentage calculated from TGA turns out to be 19.6%, which is commensurate with the UV data.

3.3. Kinetic Experiments of Drug Loading. To gain a further understanding of NFX encapsulation in MIL-100(Fe), we performed kinetic experiments (Figure 6). Relatively fast drug uptake was observed as the maximum drug (nearly 15%) was adsorbed in 8 h of its total drug capacity of 20%. We obtained a total drug loading of 20% in about 60 h. NFX encapsulation in MIL-100(Fe) is thus a prolonged process and reaches saturation in 60 h.

3.4. In Vitro Drug Release Study of NFX@MIL-100(Fe). The in vitro drug release study of NFX was carried out using freshly prepared PBSs of two different pHs, pH 7.4 and 6.5, as

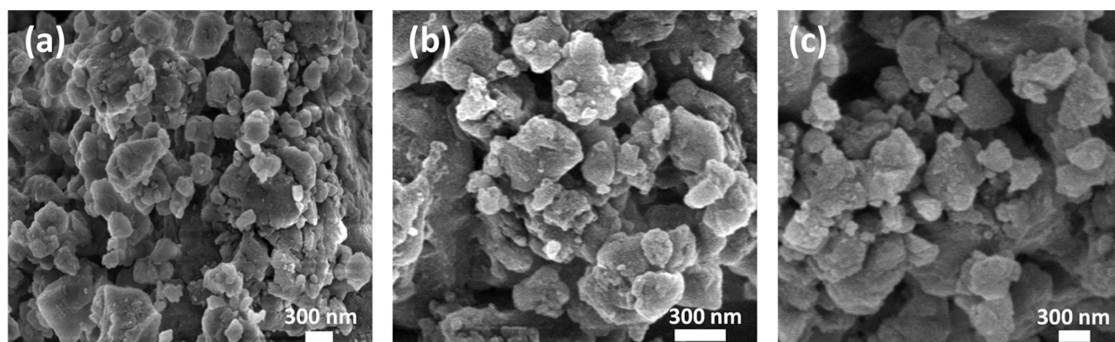


Figure 4. FESEM characterization of (a) MIL-100(Fe), (b) NFX@MIL-100(Fe), and (c) PEG{NFX@MIL-100(Fe)}.

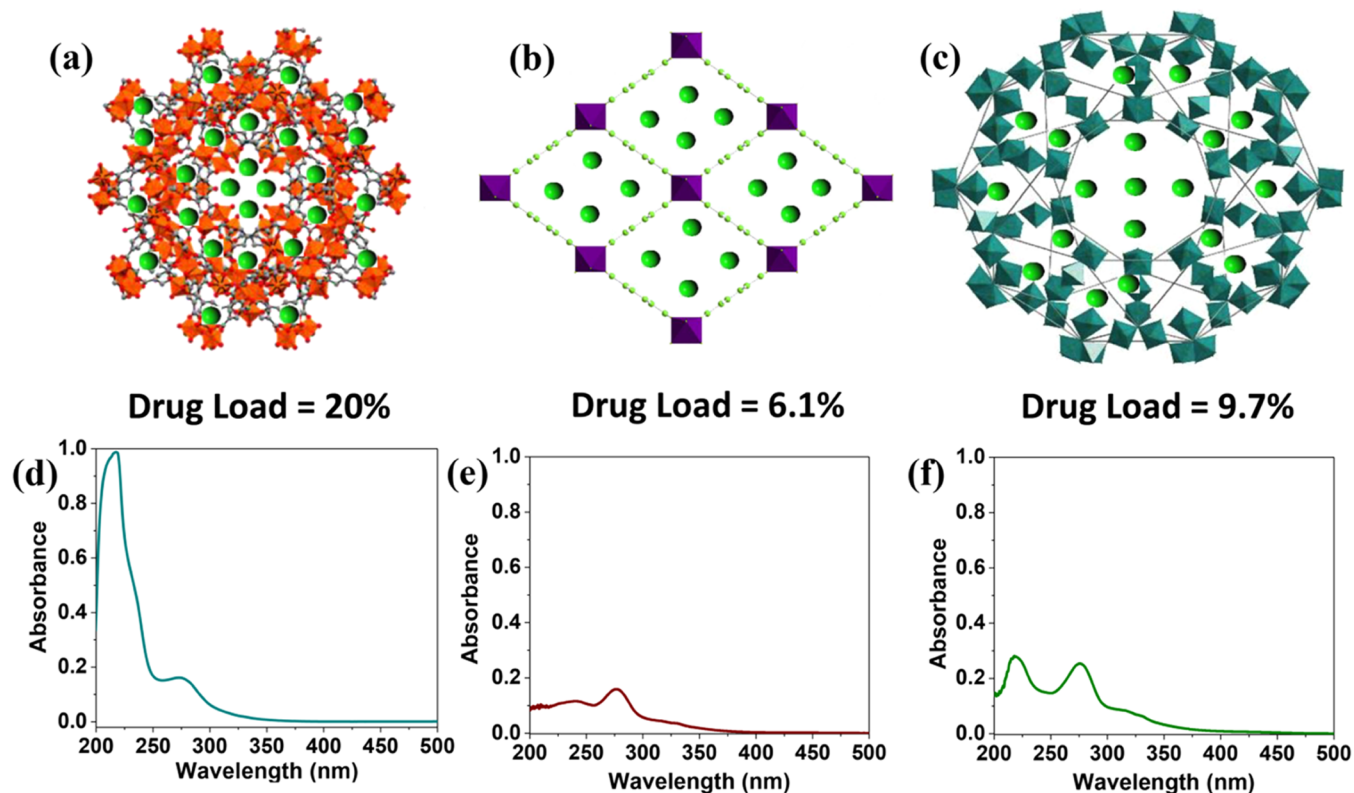


Figure 5. Schematic representation of NFX encapsulation in MIL-100(Fe) (a), MIL-53(Fe) (b), and MIL-101(Fe)_{NH₂} (c), and the corresponding UV-vis absorption spectra of NFX@MIL-100(Fe) (d), NFX@MIL-53(Fe) (e), and NFX@MIL-101(Fe)_{NH₂} (f). The experiments suggest that MIL-100(Fe) is the best candidate for loading NFX.

release media, which provided simulated biological environments (Figures S9–S12).

The two pHs were chosen keeping in mind the pH of blood (7.4) and the pH of the prostate (6.5), where the distribution of NFX is prominent. The release of NFX from the DDSs at pHs 7.4 and 6.5 is shown in Figures 7 and 8, respectively. It can be seen from the graphs in both figures that the release of NFX from NFX@MIL-100(Fe) is gradual over time. At pH 7.4, the majority of the release occurs within around 24 h, while we could still detect a small but not insignificant release up to 60 h while reaching saturation (~58%). At pH 6.5, in the case of NFX@MIL-100(Fe), the release profile is similar. However, a higher amount of drug (~72%) can be seen released from the DDS. We say that this release of NFX, from NFX@MIL-100(Fe) at both pHs, is sustained.

3.5. Coating of NFX@MIL-100(Fe) with PEG and the In Vitro Drug Release Study of PEG{NFX@MIL-100(Fe)}. In

order to get a better control of the release of NFX, we planned to coat the drug-loaded DDS, NFX@MIL-100(Fe), with a biocompatible polymer, poly(ethylene glycol) (PEG). PEG is a homopolymer of ethylene glycol, formed by the condensation of ethylene oxide and water. They possess several properties such as nontoxicity, odorless, hydrophilicity, nonvolatile, etc. The PEG coating creates a hydrophilic shield on MOF particles that will eventually protect the MOF from the external environment and impart colloidal stability to the MOF–drug system.⁴¹ The use of PEG for coating compounds is widely reported in the MOF literature.^{43–45} To achieve the PEG coating, NFX@MIL-100(Fe) was dispersed in a 1:1 (v/v) water–ethanol solution, and then, a known amount of PEG was added to it. The mixture was sonicated for 10 min to get PEG{NFX@MIL-100(Fe)}. The PEG coating was confirmed by FTIR spectroscopy (Figure S13). PEG may attach to MIL-100(Fe) through covalent bonding, resulting in the coating of

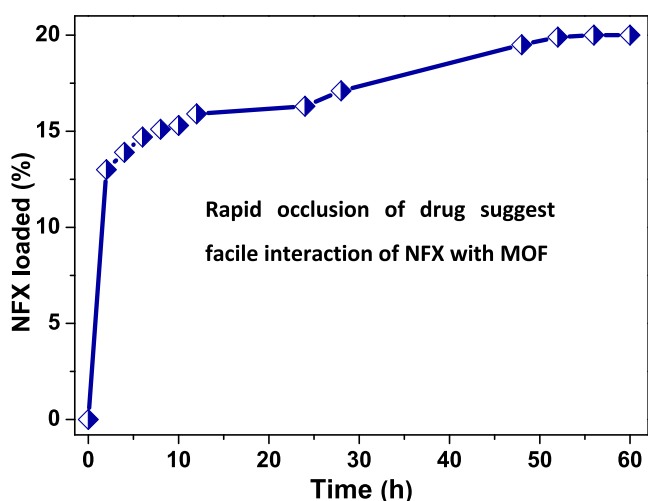


Figure 6. Time-dependent NFX loading in MIL-100(Fe) showing a rapid occlusion of the drug in MOF and then almost saturating after 50 h.

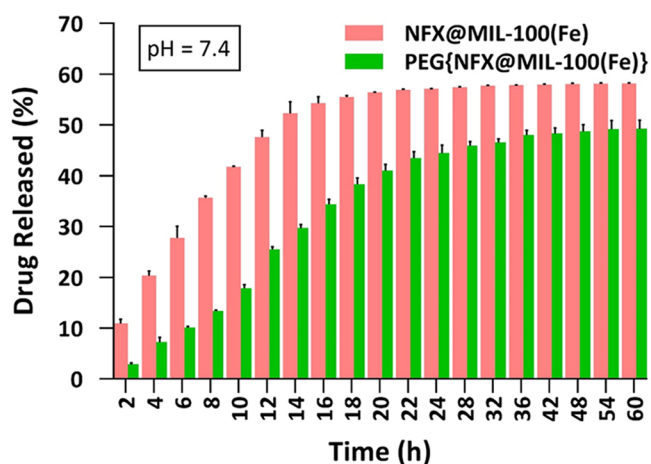


Figure 7. Drug release profile of NFX@MIL-100(Fe) [pink bars] and PEG{NFX@MIL-100(Fe)} [green bars] at pH 7.4. Better control of cumulative drug release in the case of PEG{NFX@MIL-100(Fe)} can be seen at the very beginning, e.g., at 2 h, 3% in contrast to 11% in NFX@MIL-100(Fe). Similarly, at 6, 10, and 14 h, 10, 18, and 30% in contrast to 26, 41, and 53%, respectively.

MOF particles.⁴⁵ The NFX release from the PEG-coated DDSs, PEG{NFX@MIL-100(Fe)}, is shown in Figure 7 (green bars) and Figure 8 (green bars). It is very encouraging to see that the release of NFX at both pHs has slowed down in comparison to the release from NFX@MIL-100(Fe). In the beginning, graphs in Figures 7 and 8 show a clearer view of the difference in NFX release in NFX@MIL-100(Fe) and PEG{NFX@MIL-100(Fe)}. At pH 7.4, only 3% NFX is released compared to 11% in 2 h, while 30% of the drug is released in 14 h compared to 53% in NFX@MIL-100(Fe). These observations clearly indicate a greater control of drug release in the PEG-coated DDS, PEG{NFX@MIL-100(Fe)}. A similar trend is observed at pH 6.5, where 9% drug is released from NFX@MIL-100(Fe) compared to 15% in 2 h, while only 47% drug is released in 14 h compared to 65% from the uncoated DDS. The process of drug release from PEG{NFX@MIL-100(Fe)} is sustained. However, a better control is obtained with the PEG coating. The PEG coating enhances the dispersion of the drug@MOF system compared

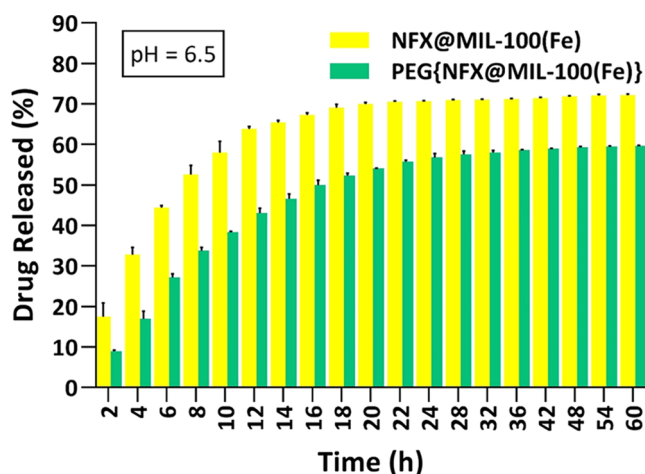


Figure 8. Drug release profile of NFX@MIL-100(Fe) [yellow bars] and (b) PEG{NFX@MIL-100(Fe)} [green bars] at pH 6.5. A better control of cumulative drug release in the case of PEG{NFX@MIL-100(Fe)} can be seen at the very beginning, e.g., at 2 h, 9% in contrast to 15% in NFX@MIL-100(Fe). Similarly, at 6, 10, and 14 h, 26, 38, and 47% in contrast to 45, 60, and 65%, respectively.

to the noncoated drug@MOF. However, due to the presence of the PEG coating on the particles of MOF, the diffusion of NFX in PBS will be comparatively slow. Apart from this, the release of the drug may also be accompanied by the degradation of DDSs, which takes place by the replacement of trimesate anions with phosphate anions of PBS.⁴⁶ However, in the case of PEG coating, the polymer shields the incoming anions or creates steric hindrance, which prolongs the MOF degradation and hence causes a slow release of the drug from the MOF. A sustained and controlled release of the drug is helpful in the case of NFX, as the drug has very poor aqueous solubility and a fast precipitation rate. Moreover, the undesired loss of the drug could be reduced significantly within physiological conditions by allowing the drug to release from the DDS, PEG{NFX@MIL-100(Fe)}. Incremental release up to 60 h might be attributed to the release of drugs from the inner channels of the MOF due to its degradation in PBS. From these studies, we can conclude that MIL-100(Fe) MOF can be proved as an excellent candidate for the loading of NFX and further its sustained and controlled release after coating with PEG.

3.6. Cell Viability Assessment. To establish the applicability of the designed DDSs, we ventured to study the cytotoxicity of all of the compounds. The cytotoxicity of MIL-100(Fe), NFX@MIL-100(Fe), and PEG{NFX@MIL-100(Fe)} was examined by the MTT assay on Vero-2 cells. Cell survival was tested to determine the cytotoxic effect of the test compounds. After cell recovery, Vero-2 cells were counted using a hemocytometer and seeded 10^4 cells per well into a 96-well plate and incubated for 24 h for adherence at 37 °C with 5% CO₂.⁴⁷ Next day, media was replaced, and the cells were treated with serially diluted concentrations (2000, 200, 20, 2, 0.2, 0.02, and 0.002 μg/mL) of the test compounds and incubated for 48 h. Cells with no test compound were used as control. After incubation for 48 h, media was removed by suction, and 20 μL of 5 mg/mL MTT was added with complete media to each well and incubated further for 4 h at 37 °C. Subsequently, the media was discarded from the wells and 100 μL of DMSO was added to each well for dissolving the formed formazan crystals and incubated for 30 min.

Finally, the absorbance was measured at 540 nm using a multiplate reader.

The results of cytotoxicity of all test compounds at different concentrations by the MTT assay are shown in Figure 9. It

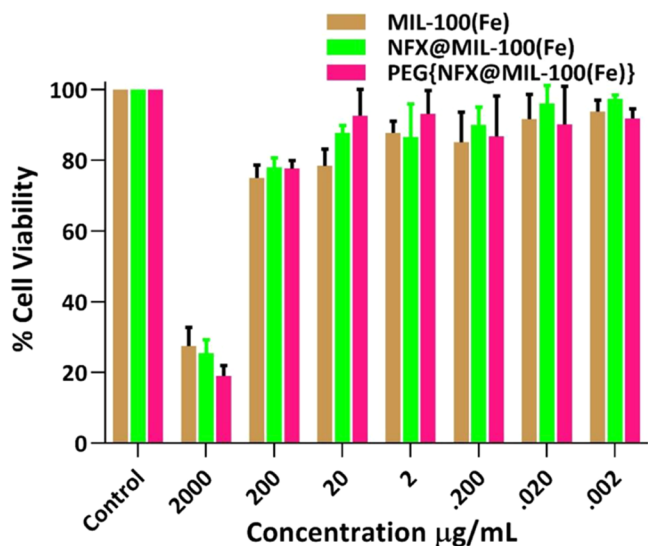


Figure 9. Cell viability assessment: the effect of test compounds MIL-100(Fe), NFX@MIL-100(Fe), and PEG{NFX@MIL-100(Fe)} at different concentrations (2000, 200, 20, 2, 0.2, 0.02, and 0.002 µg/mL). No significant cytotoxicity was observed at 200 µg/mL. Significant cytotoxicity was observed only at 2000 µg/mL.

reveals an approximate >75% cell viability after 48 h treatment at the higher concentration (200 µg/mL), which indicates that MOF and DDSs are nontoxic at the experimental doses, suggesting that the MOF and designed formulations show no cytotoxic effects on the Vero-2 cells. The toxicity of test compounds is significantly cytotoxic only at 2000 µg/mL concentration.

4. CONCLUSIONS

In summary, we have employed a new approach for delivering norfloxacin by using a biocompatible MOF, MIL-100(Fe), and its porous platform. Norfloxacin, a BCS class IV drug, was chosen for the study, as it has low solubility issues in aqueous medium. The drug was successfully loaded on the MOF and its release study was carried out in PBS at two different pHs, 7.4 and 6.5. A desired sustained and controlled release was achieved at both pHs by coating the drug-loaded MOF with PEG. Further, we carried out cytotoxicity studies of the systems through the MTT assay, which showed insignificant toxicity. The proposed drug delivery system is easy to synthesize and process and is biocompatible. We believe our work will pave the way toward the incremental and controlled release of other poorly soluble drugs from the porous platforms of judiciously selected MOFs. This facile and easy approach will be effective in enhancing the performance of drug molecules that have poor solubility. More studies on other drug molecules are underway in our lab and will be reported in due course.

■ ASSOCIATED CONTENT

Supporting Information

The Supporting Information is available free of charge at <https://pubs.acs.org/doi/10.1021/acsomega.3c02418>.

Materials and methods; experimental details; scheme; IR spectra; TGA curves; and UV–visible curves (PDF)

■ AUTHOR INFORMATION

Corresponding Authors

Anindita Chakraborty – Department of Chemistry, School of Basic Sciences, Central University of Haryana, Mahendergarh 123031 Haryana, India; orcid.org/0000-0001-5109-3890; Email: achakraborty@cuh.ac.in

Prakash Kanoo – Department of Chemistry, School of Basic Sciences, Central University of Haryana, Mahendergarh 123031 Haryana, India; orcid.org/0009-0009-0798-7964; Email: prakashkanoo@cuh.ac.in

Authors

Preeti Yadav – Department of Chemistry, School of Basic Sciences, Central University of Haryana, Mahendergarh 123031 Haryana, India

Sarita Kumari – Department of Chemistry, School of Basic Sciences, Central University of Haryana, Mahendergarh 123031 Haryana, India

Anand Yadav – Department of Chemistry, School of Basic Sciences, Central University of Haryana, Mahendergarh 123031 Haryana, India

Priya Bhardwaj – Department of Biochemistry, School of Interdisciplinary and Applied Sciences, Central University of Haryana, Mahendergarh 123031 Haryana, India

Mulaka Maruthi – Department of Biochemistry, School of Interdisciplinary and Applied Sciences, Central University of Haryana, Mahendergarh 123031 Haryana, India

Complete contact information is available at:

<https://pubs.acs.org/10.1021/acsomega.3c02418>

Notes

The authors declare no competing financial interest.

■ ACKNOWLEDGMENTS

P.K. is grateful to Science and Engineering Research Board (SERB), New Delhi, for an Early Career Research Grant (ECR/2017/000038). A.C. is grateful to Department of Science and Technology (DST), New Delhi, India, for an INSPIRE Faculty Fellowship (DST/INSPIRE/04/2020/001603). P.K. and A.C. thankfully acknowledge the infrastructural support and characterization facility at Central University of Haryana, Mahendergarh. P.Y. and S.K. thank CSIR, New Delhi, for senior research fellowships. The authors gratefully acknowledge Dr. Ritesh Haldar of TIFR Hyderabad, Central Instrumentation Centre of GJU, Hisar, and Mr. Mritunjay Arora of Anton Paar India Pvt. Ltd. for helping with measurements.

■ REFERENCES

- (1) Agostoni, V.; Anand, R.; Monti, S.; Hall, S.; Maurin, G.; Horcajada, P.; Serre, C.; Bouchemala, K.; Gref, R. Impact of Phosphorylation on the Encapsulation of Nucleoside Analogues Within Porous Iron(III) Metal–Organic Framework MIL-100(Fe) Nanoparticles. *J. Mater. Chem. B* **2013**, *1*, 4231–4242.
- (2) Wang, L.; Zheng, M.; Xie, Z. Nanoscale Metal–Organic Frameworks for Drug Delivery: A Conventional Platform with New Promise. *J. Mater. Chem. B* **2018**, *6*, 707–717.
- (3) Della Rocca, J.; Liu, D.; Lin, W. Nanoscale Metal–Organic Frameworks for Biomedical Imaging and Drug Delivery. *Acc. Chem. Res.* **2011**, *44*, 957–968.

- (4) Souza, B. E.; Tan, J.-C. Mechanochemical Approaches Towards the In Situ Confinement of 5-FU Anti-Cancer Drug Within MIL-100(Fe) Metal–Organic Framework. *CrystEngComm* **2020**, *22*, 4526–4530.
- (5) Horcajada, P.; Serre, C.; Regí, M. V.; Sebba, M.; Taulelle, F.; Férey, G. Metal–Organic Frameworks as Efficient Materials for Drug Delivery. *Angew. Chem., Int. Ed.* **2006**, *45*, 5974–5978.
- (6) Horcajada, P.; Chalati, T.; Serre, C.; Gillet, B.; Sebrie, C.; Baati, T.; Eubank, J.; Heurtaux, D.; Clayette, P.; Kreuz, C.; Chang, J.; Hwang, Y.; Marsaud, V.; Bories, P.; Cynober, L.; Gil, S.; Férey, G.; Couvreur, P.; Gref, R. Porous Metal–Organic-Framework Nanoscale Carriers as a Potential Platform for Drug Delivery and Imaging. *Nat. Mater.* **2010**, *9*, 172–178.
- (7) Anand, R.; Borghi, F.; Manoli, F.; Manet, I.; Agostoni, V.; Reschiglian, P.; Gref, R.; Monti, S. Host–Guest Interactions in Fe(III)-Trimesate MOF Nanoparticles Loaded with Doxorubicin. *J. Phys. Chem. B* **2014**, *118*, 8532–8539.
- (8) Taylor, D. The Pharmaceutical Industry and the Future of Drug Development. In *Pharmaceuticals in the Environment*; Hester, R. E.; Harrison, R. M., Eds.; The Royal Society of Chemistry: London, 2016; pp 1–33.
- (9) Bhattacharya, B.; Mondal, A.; Soni, S. R.; Das, S.; Bhunia, S.; Raju, K. B.; Ghosh, A.; Reddy, C. M. Multidrug Salt Forms of Norfloxacin with Non-Steroidal Anti-Inflammatory Drugs: Solubility and Membrane Permeability Studies. *CrystEngComm* **2018**, *20*, 6420–6429.
- (10) Parsaei, M.; Akhbari, K. MOF-801 as a Nanoporous Water-Based Carrier System for In Situ Encapsulation and Sustained Release of 5-FU for Effective Cancer Therapy. *Inorg. Chem.* **2022**, *61*, 5912–5925.
- (11) Zhang, P.; Li, Y.; Tang, Y.; Shen, H.; Li, J.; Yi, Z.; Ke, Q.; Xu, H. Copper-Based Metal–Organic Framework as a Controllable Nitric Oxide-Releasing Vehicle for Enhanced Diabetic Wound Healing. *ACS Appl. Mater. Interfaces* **2020**, *12*, 18319–18331.
- (12) Hu, Z.; Qiao, C.; Xia, Z.; Li, F.; Han, J.; Wei, Q.; Yang, Q.; Xie, G.; Chen, S.; Gao, S. A Luminescent Mg-Metal–Organic Framework for Sustained Release of 5-Fluorouracil: Appropriate Host–Guest Interaction and Satisfied Acid–Base Resistance. *ACS Appl. Mater. Interfaces* **2020**, *12*, 14914–14923.
- (13) Karimi Alavijeh, R.; Akhbari, K. Biocompatible MIL-101(Fe) as a Smart Carrier with High Loading Potential and Sustained Release of Curcumin. *Inorg. Chem.* **2020**, *59*, 3570–3578.
- (14) Sava Gallis, D. F.; Butler, K. S.; Agola, J. O.; Pearce, C. J.; McBride, A. A. Antibacterial Countermeasures via Metal–Organic Framework-Supported Sustained Therapeutic Release. *ACS Appl. Mater. Interfaces* **2019**, *11*, 7782–7791.
- (15) Wang, H.-L.; Yeh, H.; Li, B.-H.; Lin, C.-H.; Hsiao, T.-C.; Tsai, D.-H. Zirconium-Based Metal–Organic Framework Nanocarrier for the Controlled Release of Ibuprofen. *ACS Appl. Nano Mater.* **2019**, *2*, 3329–3334.
- (16) Cai, W.; Wang, J.; Chu, C.; Chen, W.; Wu, C.; Liu, G. Metal–Organic Framework-Based Stimuli-Responsive Systems for Drug Delivery. *Adv. Sci.* **2019**, *6*, No. 1801526.
- (17) Rojas, S.; Colinet, I.; Cunha, D.; Hidalgo, T.; Salles, F.; Serre, C.; Guillou, N.; Horcajada, P. Toward Understanding Drug Incorporation and Delivery from Biocompatible Metal–Organic Frameworks in View of Cutaneous Administration. *ACS Omega* **2018**, *3*, 2994–3003.
- (18) Lin, S.; Liu, X.; Tan, L.; Cui, Z.; Yang, X.; Yeung, K. W. K.; Pan, H.; Wu, S. Porous Iron-Carboxylate Metal–Organic Framework: A Novel Bioplateform with Sustained Antibacterial Efficacy and Nontoxicity. *ACS Appl. Mater. Interfaces* **2017**, *9*, 19248–19257.
- (19) Bhattacharjee, A.; Purkait, M. K.; Gumma, S. Loading and Release of Doxorubicin Hydrochloride from Iron(III) Trimesate MOF and Zinc Oxide Nanoparticle Composites. *Dalton Trans.* **2020**, *49*, 8755–8763.
- (20) Zhou, H.-C.; Long, J. R.; Yaghi, O. M. Introduction to Metal–Organic Frameworks. *Chem. Rev.* **2012**, *112*, 673–674.
- (21) Zhou, H.-C. J.; Kitagawa, S. Metal–Organic Frameworks (MOFs). *Chem. Soc. Rev.* **2014**, *43*, 5415–5418.
- (22) Chen, Z.; Kirlikovali, K. O.; Li, P.; Farha, O. K. Reticular Chemistry for Highly Porous Metal–Organic Frameworks: The Chemistry and Applications. *Acc. Chem. Res.* **2022**, *55*, 579–591.
- (23) Erkartal, M.; Sen, U. Boronic Acid Moiety as Functional Defect in UiO-66 and Its Effect on Hydrogen Uptake Capacity and Selective CO₂ Adsorption: A Comparative Study. *ACS Appl. Mater. Interfaces* **2018**, *10*, 787–795.
- (24) Millward, A. R.; Yaghi, O. M. Metal–Organic Frameworks with Exceptionally High Capacity for Storage of Carbon Dioxide at Room Temperature. *J. Am. Chem. Soc.* **2005**, *127*, 17998–17999.
- (25) Yadav, A.; Kumari, S.; Yadav, P.; Hazra, A.; Chakraborty, A.; Kanoo, P. Open Metal Site (OMS)-Inspired Investigation of Adsorption and Catalytic Functions in a Porous Metal–Organic Framework (MOF). *Dalton Trans.* **2022**, *51*, 15496–15506.
- (26) Han, Q.; Dong, Y.; Xu, C.; Hu, Q.; Dong, C.; Liang, X.; Ding, Y. Immobilization of Metal–Organic Framework MIL-100(Fe) on the Surface of BiVO₄: A New Platform for Enhanced Visible-Light-Driven Water Oxidation. *ACS Appl. Mater. Interfaces* **2020**, *12*, 10410–10419.
- (27) Duan, S.; Li, J.; Liu, X.; Wang, Y.; Zeng, S.; Shao, D.; Hayat, T. HF-Free Synthesis of Nanoscale Metal–Organic Framework NMIL-100(Fe) as an Efficient Dye Adsorbent. *ACS Sustainable Chem. Eng.* **2016**, *4*, 3368–3378.
- (28) Orellana-Tavra, C.; Tavra, C. O.; Marshall, R. J.; Baxter, E. F.; Lazaro, I. A.; Tao, A.; Cheetham, A. K.; Cheetham, A. K.; Forgan, R. S.; Forgan, R. S.; Jimenez, D. F. Drug Delivery and Controlled Release from Biocompatible Metal–Organic Frameworks Using Mechanical Amorphization. *J. Mater. Chem. B* **2016**, *4*, 7697–7707.
- (29) Yang, C.-X.; Liu, C.; Cao, Y.-M.; Yan, X.-P. Metal–Organic Framework MIL-100(Fe) for Artificial Kidney Application. *RSC Adv.* **2014**, *4*, 40824–40827.
- (30) Zhou, Y.; Liu, L.; Cao, Y.; Yu, S.; He, C.; Chen, X. A Nanocomposite Vehicle Based on Metal–Organic Framework Nanoparticle Incorporated Biodegradable Microspheres for Enhanced Oral Insulin Delivery. *ACS Appl. Mater. Interfaces* **2020**, *12*, 22581–22592.
- (31) Rezaei, M.; Abbasi, A.; Varshochian, R.; Dinarvand, R.; Tehrani, M. J. NanoMIL-100(Fe) Containing Docetaxel for Breast Cancer Therapy. *Artif. Cells, Nanomed., Biotechnol.* **2018**, *46*, 1390–1401.
- (32) Zhao, J.; Yin, F.; Ji, L.; Wang, C.; Shi, C.; Liu, X.; Yang, H.; Wang, X.-B.; Kong, L.-Y. Development of a Tau-Targeted Drug Delivery System Using a Multifunctional Nanoscale Metal–Organic Framework for Alzheimer’s Disease Therapy. *ACS Appl. Mater. Interfaces* **2020**, *12*, 44447–44458.
- (33) Basavojju, S.; Bostrom, S.; Velaga, S. P. Pharmaceutical Cocrystal and Salts of Norfloxacin. *Cryst. Growth Des.* **2006**, *6*, 2699–2708.
- (34) Gopi, S. P.; Ganguly, S.; Desiraju, G. R. A Drug–Drug Salt Hydrate of Norfloxacin and Sulfathiazole: Enhancement of in Vitro Biological Properties via Improved Physicochemical Properties. *Mol. Pharmaceutics* **2016**, *13*, 3590–3594.
- (35) Florindo, C.; Costa, A.; Matos, C.; Nunes, S. L.; Matias, A. N.; Duarte, C. M. M.; Rebelo, L. P. N.; Branco, L. C.; Marrucho, I. M. Novel Organic Salts Based on Fluoroquinolone Drugs: Synthesis, Bioavailability and Toxicological Profiles. *Int. J. Pharm.* **2014**, *469*, 179–189.
- (36) Dos Santos, I.; Fawaz, F.; Lagueny, A. M.; Bonini, F. Improvement of Norfloxacin Oral Bioavailability by EDTA and Sodium Caprate. *Int. J. Pharm.* **2003**, *260*, 1–4.
- (37) Dhaneshwar, S.; Tewaria, K.; Joshi, S.; Godbole, D.; Ghosh, P. Diglyceride Prodrug Strategy for Enhancing the Bioavailability of Norfloxacin. *Chem. Phys. Lipids* **2011**, *164*, 307–313.
- (38) Bhattacharjee, A.; Gumma, S.; Purkait, M. K. Fe₃O₄ promoted metal organic framework MIL-100(Fe) for the controlled release of doxorubicin hydrochloride. *Microporous Mesoporous Mater.* **2018**, *259*, 203–210.

- (39) Mohanta, V.; Madras, G.; Patil, S. Layer-by-Layer Assembled Thin Film of Albumin Nanoparticles for Delivery of Doxorubicin. *J. Phys. Chem. C* **2012**, *116*, 5333–5341.
- (40) Thi, H. P. N.; Ninh, H. D.; Tran, C. V.; Le, B. T.; Bhosale, S. V.; La, D. D. Size-Control and Surface Modification of Flexible Metal-Organic Framework MIL-53(Fe) by Polyethyleneglycol for 5-Fluorouracil Anticancer Drug Delivery. *ChemistrySelect* **2019**, *4*, 2333–2338.
- (41) Barjasteh, M.; Vossoughi, M.; Bagherzadeh, M.; Bagheri, P. K. Green synthesis of PEG-Coated MIL-100(Fe) for Controlled Release of Dacarbazine and its Anticancer Potential Against Human Melanoma Cells. *Int. J. Pharm.* **2022**, *618*, No. 121647.
- (42) Bauer, S.; Serre, C.; Devic, T.; Horcajada, P.; Marrot, J.; Fe'rey, G.; Stock, N. High-Throughput Assisted Rationalization of the Formation of Metal Organic Frameworks in the Iron(III) Amino-terephthalate Solvothermal System. *Inorg. Chem.* **2008**, *47*, 7568–7576.
- (43) Agostoni, V.; Horcajada, P.; Noiray, M.; Malanga, M.; Aykaç, A.; Jicsinszky, L.; Berenguel, A. V.; Semiramoth, N.; Mahammed, S. D.; Nicolas, V.; Martineau, C.; Taulelle, F.; Vigneron, J.; Etcheberry, A.; Serre, C.; Gref, R. A “green” Strategy to Construct Non-Covalent, Stable and Bioactive Coatings on Porous MOF Nanoparticles. *Sci. Rep.* **2015**, *5*, No. 7925.
- (44) Abánades Lázaro, I.; Haddad, S.; Muñoz, J. M. R.; Tavra, C. O.; Pozo, Vd.; Jimenez, D. F.; Forgan, R. S. Mechanistic Investigation into the Selective Anticancer Cytotoxicity and Immune System Response of Surface-Functionalized, Dichloroacetate-Loaded, UiO-66 Nanoparticles. *ACS Appl. Mater. Interfaces* **2018**, *10*, 5255–5268.
- (45) Zimpel, A.; Preiß, T.; Röder, R.; Engelke, H.; Ingris, M.; Peller, M.; Rädler, J. O.; Wagner, E.; Bein, T.; Lächelt, U.; Wuttke, S. Imparting Functionality to MOF Nanoparticles by External Surface Selective Covalent Attachment of Polymers. *Chem. Mater.* **2016**, *28*, 3318–3326.
- (46) Giménez-Marqués, M.; Bellido, E.; Berthelot, T.; Simón-Yarza, T.; Hidalgo, T.; Simón-Vázquez, R.; González-Fernández, A.; Avila, J.; Asensio, M. C.; Gref, R.; Couvreur, P.; Serre, C.; Horcajada, P. GraftFast Surface Engineering to Improve MOF Nanoparticles Furtiveness. *Small* **2018**, *14*, No. 1801900.
- (47) van Meerloo, J.; Kaspers, G. J.; Cloos, J. Cell Sensitivity Assays: The MTT Assay. In *Cancer Cell Culture, Methods in Molecular Biology*; Springer, 2011; Vol. 731, pp 237–45.